Astron. Astrophys. 336, 490–502 (1998)

ASTRONOMY AND ASTROPHYSICS

Brown dwarfs and very low-mass stars in the Pleiades cluster: a deep wide-field imaging survey⋆

J. Bouvier[1], **J.R. Stauffer**[2], **E.L. Martín**[3,4], **D. Barrado y Navascués**[3], **B. Wallace**[5], **and V.J.S. Béjar**[4]

[1] Laboratoire d'Astrophysique, Observatoire de Grenoble, Université Joseph Fourier, B.P. 53, F-38041 Grenoble Cedex 9, France (jbouvier@laog.obs.ujf-grenoble.fr, http://gag.observ-gr.fr/liens/starform/formation.html)
[2] Harvard-Smithsonian Center for Astrophysics, 60 Garden Street, Cambridge, MA 02138, USA
[3] University of California at Berkeley, 601 Campbell Hall, Berkeley, CA 94720, USA
[4] Instituto de Astrofísica de Canarias, E-38200 La Laguna, Tenerife, Spain
[5] University of Victoria, B.C., Canada

Received 20 March 1998 / Accepted 29 May 1998

Abstract. We have performed a deep, wide-field imaging survey of the Pleiades cluster (Melotte 22) in the R and I-bands to search for very low-mass stars and brown dwarfs. The survey extends over ∼2.5 square degrees around the cluster's center down to a ∼90% completeness limit of R∼23 and I∼22. We find 26 objects whose location in the (I, R-I) color–magnitude diagram is consistent with them being Pleiades members. Of these, 17 have extremely red (R-I) colors and low I luminosity, which make them prime brown dwarf candidates. We present the luminosity function of the Pleiades cluster down to M_I ∼15. Using current-generation theoretical models, we compute the mass of the brown dwarf candidates which is found to range from the hydrogen-burning limit down to about $0.045\mathcal{M}_\odot$. Based on these results, a preliminary estimate of the Pleiades mass function is presented. While the stellar portion of the Pleiades mass function is well approximated by the log-normal IMF of Miller & Scalo (1979), the substellar part of it is found to be slightly higher than predicted by Miller & Scalo's IMF. In a log-log plot, the IMF is found to be still rising in the substellar domain, with a slope consistent with $dN/dM \sim M^{-0.6}$ if a power-law functional form is assumed. We estimate a total of about 250 objects below the hydrogen burning mass limit in the Pleiades which nevertheless make up only a few per cent of the mass of the cluster.

Key words: stars: low-mass, brown dwarfs – stars: luminosity function, mass function – Galaxy: open clusters and associations: individual: Pleiades = Melotte 22 – Galaxy: open clusters and associations: general

1. Introduction

Imaging surveys for brown dwarfs have generally targeted young open clusters or star-forming regions because they provide context for any identified brown dwarf and because brown dwarfs are brighter and warmer when they are young. Based either on the number of papers published or on the number of confirmed brown dwarfs identified, by far the most productive of these regions has been the Pleiades open cluster. Astronomers have voted with their telescope time to make the Pleiades the prime hunting ground for brown dwarfs because its properties are closest to the ideal one would desire. Those properties include: (a) its age of about 100 Myr, which is old enough so that the lithium test (Rebolo, Martín and Magazzù 1992) is useful but young enough so that objects at the hydrogen burning mass limit (HBML) are still relatively warm and hence easily detected in the optical where large format detectors are available; (b) its distance of about 125 pc, which is near enough so that the apparent magnitude of the HBML is relatively bright and optical imaging surveys can detect objects below the HBML even with relatively small telescopes; (c) its "richness", with more than 800 catalogued members, and (d) its relatively high galactic latitude, which minimizes the background density of old disk dwarfs and entirely avoids having to distinguish brown dwarf candidates from heavily reddened, distant giants.

Imaging surveys to detect brown dwarfs in the Pleiades were begun almost a decade ago. However, for a number of years interpretation of those surveys was problematic because theoretical evolutionary tracks were not reliable enough to confidently demarcate the location of the HBML at Pleiades age (Stauffer et al.1994) and there was no predicted signpost that denoted an object as a brown dwarf based on information obtainable from low resolution spectroscopy or photometric colors. This unsatisfactory state of affairs was resolved by the detection of lithium in a high-resolution spectrum of one of the Pleiades brown dwarf candidates, PPL 15, by Basri, Marcy & Graham (1996) using the Keck I telescope. Non-detection of a number of brighter Pleiades members (Marcy, Basri & Graham 1994; Martín, Rebolo & Magazzù 1994; Oppenheimer et al.1997) and subsequent detection of lithium in two other Pleiades brown dwarf candidates (Rebolo et al.1996) now require the HBML to be somewhere in the range $17.5 \leq I \leq 18.5$, and suggest that

Send offprint requests to: J. Bouvier

⋆ Based on observations obtained at the Canada-France-Hawaii Telescope and the KPNO 4m telescope.

Table 1. Imaging surveys for Pleiades brown dwarfs

Survey	Area	Completeness Limit	# of Suggested Brown Dwarfs	# of Confirmed Brown Dwarfs	# of Remaining Candidates
Jameson & Skillen (1989)	250 sq. arcmin.	I ∼17	7	0	0
Stauffer et al.(1989)	900 sq. arcmin	I ∼17.5	4	0	2
Simons & Becklin (1992)	200 sq. arcmin.	I ∼19.5	22	0	0?
Hambly, Hawkins & Jameson (1993)	21 sq. degree	I ∼17	22	0	0
Stauffer, Hamilton & Probst (1994)	800 sq. arcmin.	I ∼17.5	2	1	1
Williams et al.(1996)	400 sq. arcmin.	I ∼19	1	0	1
Zapatero, Rebolo & Martín (1997)	580 sq. arcmin.	I ∼19.5	2	2	0
Festin (1997)	180 sq. arcmin.	I ∼21.6	0	0	0
Cosburn et al.(1997)	100 sq. arcmin.	I ∼20	1	0	1
Zapatero-Osorio et al. (1997, 1998)	3600 sq. arcmin	I ∼21.2	41	0	37
Stauffer et al.(1998)	3400 sq. arcmin.	I ∼18.5	3	0	3

the Pleiades is somewhat older than previously thought, with a probable age of 100-130 Myr (Basri, Marcy & Graham 1996).

Table 1 provides a summary of the Pleiades brown dwarf imaging surveys conducted to date. The final two columns, and in particular the final column, are somewhat subjective and reflect our own personal biases or guesses in many cases. None of these Pleiades brown dwarf candidates is cool enough to have detectable photospheric methane, the most nearly certain indicator that an extrasolar, high gravity object is a brown dwarf (Burrows et al.1997). For Table 1, we therefore restrict the appelation "confirmed brown dwarf" to objects with detected lithium and with inferred effective temperatures compatible with model predictions for Pleiades age brown dwarfs. Recent models (Baraffe et al. 1998) predict that at the age of the Pleiades (120 Myr, see below), a 0.075 $M_\odot$ object will have depleted lithium by a factor of 50 relative to its initial abundance, while a 0.070 $M_\odot$ object will have depleted it only by a factor of 3. Therefore, the lithium borderline in the Pleiades closely match the HBML, located at 0.072 $M_\odot$ according to Baraffe's et al. models. Because of the detection of approximately undepleted lithium abundances in Teide 1 and Calar 3, confirmed members of the Pleiades fainter than I $\sim$ 18.5 could also be considered as confirmed brown dwarfs, but as yet the kinematic information for any of the candidate Pleiades brown dwarfs this faint is too uncertain to certify Pleiades membership. Therefore, for now, we only have $\sim$3.5 confirmed Pleiades brown dwarfs.

A general characteristic of Table 1 is that the surveys to date have either been large area but relatively shallow or deep but with relatively limited coverage. This was simply the result of the available technology - photographic plates, as used by Hambly, Hawkins and Jameson (1993=HHJ), come in quite large formats but have low quantum efficiency, while CCD's (in the optical) and InSb or HgCdTe arrays (in the near-IR) are very sensitive but have historically come in small formats. With the development of CCD-mosaic cameras on large telescopes, it has recently become possible to obtain deep and wide-field surveys in the optical. In this paper, we report the results of the first survey for Pleiades brown dwarfs conducted using a CCD-mosaic camera. We have used the Canada-France-Hawaii telescope and the UH 8Kx8K camera to survey $\sim$2.5 square degrees of the Pleiades to a completeness limit of $\sim$ 22nd magnitude in I and $\sim$ 23rd in R. We have identified more than 15 brown dwarf candidates in these images, and provide their coordinates, I magnitudes and $(R\text{-}I)_c$ colors, and finding charts for these objects. We also discuss our initial attempts to constrain the Pleiades mass function below the HBML using these data.

2. Observations and data reduction

We have obtained deep images in the R- and I-bands of ten $30'$ $\times$ $30'$ fields in the Pleiades using the University of Hawaii 8K CCD mosaic at the prime focus of the Canada-France-Hawaii telescope. Observations were performed from December 9 to 13, 1996, and the center coordinates of each field are listed in Table 2. The field locations relative to the brighter members of the Pleiades are shown graphically in Fig. 1. The UH 8K mosaic is an array of 8 2K$\times$4K CCDs with 15μm-size pixels, yielding a pixel scale of $0.2''$ on the sky (Cuillandre et al.1996). For each field, we obtained one 1200s exposure in the I-band and two 1800s exposures in the R-band (except for CFHT7 for which two 1200s R-exposures and two 600s I-exposures were taken). The total area covered amounts to 2.5 square degrees. The histogram of the R and I-magnitudes of stellar-like objects indicates that the survey is complete down to R_c=23.5, I_c=22.6, with limiting magnitudes of R$\simeq$25.0 and I$\simeq$23.3.

In addition to the 10 fields in the Pleiades cluster, we observed 3 fields in the older Praesepe cluster. At the age and distance of the Praesepe cluster, brown dwarf members are expected to be fainter than our detection limit. We thus use the Praesepe images as control fields for the analysis of the Pleiades fields. All of the data reduction steps for Praesepe were done in the same manner as for the Pleiades images.

To help calibrate the CFHT mosaic data, we also obtained short R and I images of the center of each mosaic field using the KPNO 4m prime focus CCD camera and a single Tektronix 2K$\times$2K CCD. We used the R and I filters from the KPNO "standard" filter set, whose R filter was designed to match the Kron-Cousins system and whose I filter is an interference filter designed by J. Mould. The 4m images are at a spatial scale of 0.47 arcsec/pixel, corresponding to a field of view of $16'$ $\times$ $16'$. The typical limiting magnitudes were I$\simeq$21.5 and R$\simeq$22.5.

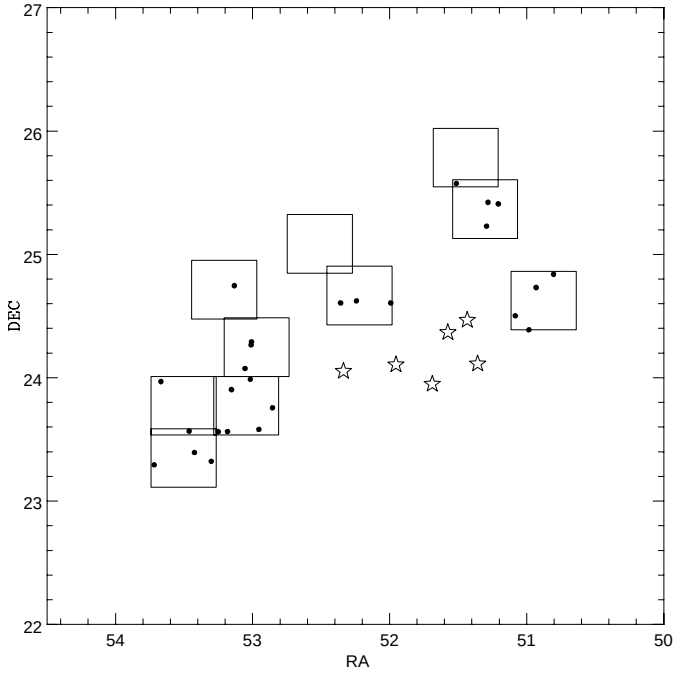

Fig. 1. Location of the 10 Pleiades fields relative to the bright Pleiades members. Filled dots show the location of the 26 Pleiades VLM and BD candidates listed in Table 3. The units are degrees on both axes.

Table 2. Field center coordinates

Field	RA(2000) (h m s)	DEC(2000) (° ′ ″)
CFHT1	03:44:38	25:22:00
CFHT2	03:48:39	24:39:59
CFHT3	03:42:46	24:37:30
CFHT5	03:51:56	24:14:56
CFHT6	03:49:55	25:05:09
CFHT7	03:52:16	23:46:22
CFHT8	03:52:58	24:42:52
CFHT10	03:54:16	23:46:21
CFHT11	03:45:15	25:47:04
CFHT13	03:54:16	23:20:59
PRAE1	08:39:48	19:22:23
PRAE2	08:37:28	19:04:00
PRAE3	08:35:50	19:25:01

At KPNO, calibration to the Cousins system was accomplished via observation of standard stars from Landolt's (1992) SA98 field and from Bessell (1990). Several very red standard stars were included in order to insure an accurate transformation to the Cousins system for the very red stars of principle interest to our program.

We employed an entirely standard data reduction procedure for the KPNO images (that is, we did not push the identification in these images as faint as possible but concentrated on obtaining accurate photometry for the brighter objects). The images were flat fielded using dome flats, and all of the object identification and photometry was done using the implementation of DAOPHOT provided in the IRAF[1] package.

We proceeded in a different manner for the CFHT data analysis. Each 30′ CFHT field consists of 8 CCD images which were reduced and analyzed separately. The images were overscan corrected and dark subtracted. In the I-band, the images were flat-field calibrated using dome flats to correct for high-spatial frequency variations in the detector response, and using smoothed sky superflats to correct for low-frequency variations (Lequeux et al.1996). In the R-band, only dome flats were available. We verified on the I-images that the low-frequency variations of dome flats and sky superflats are the same within a few percent. The 8 frames of each field were thereafter divided by the median value of their respective flat fields and multiplied by the median value of the brightest flat field in the mosaic. This renormalisation effectively corrects for the different responses of each CCD and thus leads to the same photometric zero-point for all the CCDs of the mosaic (see below).

We used the automatic object-finding algorithm from the photometric package Sextractor (Bertin & Arnouts 1996) to identify objects in the I images. More than 10^5 intensity enhancements were detected in the I images of the ten CFHT fields. PSF fitting photometry of detected objects was performed on the I images using the IRAF/DAOPHOT package. The two R-band images were shifted to the same location as the I-images and averaged. PSF photometry was performed on the resulting R images, using the I-band coordinate list as input. Once the photometry was completed, several selection criteria, based on photometric and shape parameters derived by the Sextractor and IRAF/DAOPHOT packages, were used to remove spurious objects (e.g. cosmic rays, bad pixels, bright star spikes, etc..) as well as objects whose photometry was corrupted (edge of the CCD, next to a bad column/pixel region, saturated objects). Finally, we discriminated between point-like and extended objects in the following way. The FWHM distribution of all the objects detected on every image of each field was measured. The distribution has a well-defined peak at about 0.8″ corresponding to point-like objects and a high-FWHM tail due to extended objects. For every image, we defined rather conservative lower and upper limits around the mode of the FWHM distribution within which point-like objects are to be found. Some 4 10^4 point-like objects were thus selected in the ten CFHT fields.

Photometric standard fields SA 101 and SA 92 from Landolt (1992) were observed and reduced in exactly the same way as the science images. Several exposures of SA 92 were obtained, with each image shifted in RA and/or DEC by several arcminutes, in order to observe a common set of photometric standards on every CCD of the mosaic. We thus verified that the photometric zero-point is the same for each CCD to within 0.05 magnitudes. Some 30 photometric standards from SA 92 and SA 101 were used to derive instrumental magnitudes. Because

[1] IRAF is distributed by National Optical Astronomy Observatories, which is operated by the Association of Universities for Research in Astronomy, Inc., under contract to the National Science Foundation, USA

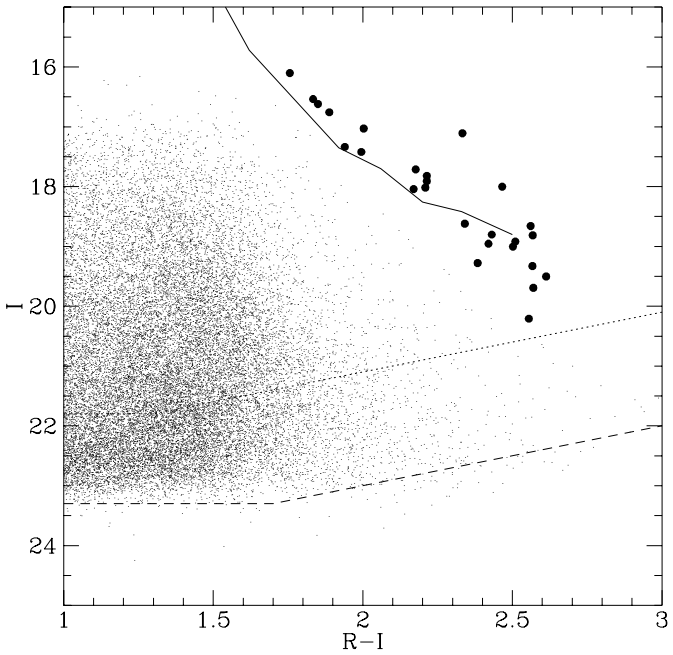

Fig. 2. Color-Magnitude diagram for point-like objects of the 10 Pleiades fields. The solid line is an empirical ZAMS, shifted to Pleiades distance and reddening. Filled dots along that line are candidates very-low mass stars and brown dwarfs of the cluster listed in Table 3. The dotted-line shows the photometric completeness limit of the survey and the dashed-one the detection limit.

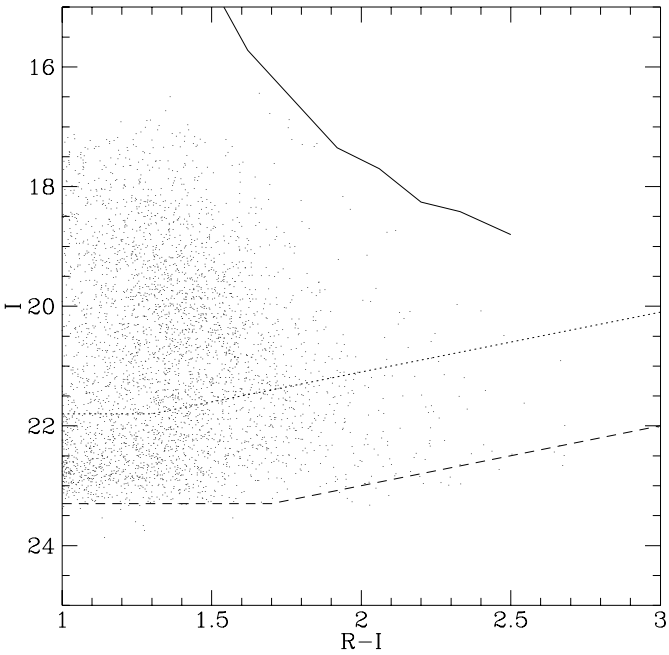

Fig. 3. Color-Magnitude diagram for point-like objects of the 3 Praesepe fields. The empirical ZAMS, shifted to Pleiades distance and reddening is shown for reference. Praesepe's main sequence should be located about 0.4 magnitudes below that of the Pleiades, based on the normally quoted distances for the two clusters.

both the R and I filters used with CFHT's UH8k mosaic are Mould and not Cousins filters, and because the Cousins standards observed at CFHT were generally much bluer than our very red program objects, an additional calibration is required to transform the CFHT provisional photometry for red objects onto the Cousins system. This calibration was done using the images obtained at KPNO. In each field (except for CFHT5 which was not observed at KPNO), some 400 stars common to CFHT and KPNO observations were used to derive the transformation equations between CFHT provisional photometry and the Cousins system. In the I-band, the transformation was merely an offset of 0.1 magnitudes with no detectable color effect. In the R-band, however, the different shape of the transmission curves of Mould and Cousins filters leads to a strong color effect for red objects. For 0.8≥(r-i)≥2.5, the derived transformation equation is:

$$R_c = r - 0.37(r - i) + 0.39$$

with an rms scatter of about 0.02 magnitudes in this color range. The equation was linearly extrapolated for objects with r-i≥2.5, i.e., R_c-I_c ≥2.0. Two very red objects, with R_c-I_c=2.5, observed both at CFHT and KPNO are found to lie within 0.1 mag of the extrapolated calibration curve. The transformation equations derived separately for each CFHT field were found to be consistent within better than 0.1 mag. Only for CFHT6 and CFHT8, which were observed through thin cirrus at CFHT, additional zero-point corrections based on the KPNO photometry were required.

The astrometric calibration of the CFHT images was done, CCD by CCD, using the IRAF/NOAO astrometric package. Typically 30 stars in every image were identified from the HST GSC and their coordinates served as a reference frame for the astrometric calibration. The triangles fitting method was used in the IRAF/astrometry package to find the astrometric solution of each image. The accuracy of the astrometric calibration is about 2 arcsec.

Several of our fields overlap by small amounts. We have used these overlap regions to estimate the completeness of our object identification. We are quite incomplete at the bright end of our sample (I∼ 16.0) due to varying saturation levels for each exposure - however, this has no affect on this paper since it only affects stars that would be $> 0.15\ \mathcal{M}_{\odot}$ in the Pleiades and these high mass objects are outside the scope of this paper. From about 1/2 magnitude above the typical saturation level to I ∼22 or R ∼23, we are > 90% complete. Comparing the total number of objects identified in one field to the stars in the overlap region of another field, we are 75% complete, with most of the missed stars being in the faintest 1.5 magnitudes of the two lists. By examination of the histogram of magnitudes for the 25% of stars not found in one field but found in the other, we derive an independent estimate of the average completeness limit for our survey of I = 21.8 and R = 23.1, somewhat brighter than we had estimated simply from examination of the histogram of the number of objects as a function of magnitude. Comparison of the overlap regions also allows us to make a test of the internal accuracy of our photometry. Down to I ∼22 or R ∼ 23, the RMS deviation between the two magnitude estimates is ≤ 5%, with

systematic offsets generally less than or of order 0.05 mag in accordance with our expectations. We believe that the external accuracy of the photometry is of order 0.1 mag, and is dominated by uncertainties in the transformation to the Cousins system, especially for very red objects.

3. Results and discussion

The (I, R-I) color-magnitude diagram of the point-like objects contained in the 10 Pleiades fields is shown in Fig. 2. For comparison, the color-magnitude diagram of the objects contained in the 3 Praesepe control fields is shown in Fig. 3. The solid curve shown in Fig. 2 is an empirical ZAMS derived from nearby field stars with tabulated Cousin's system R-I colors provided by Leggett (1992) and Bessell (1990). To place this ZAMS onto Fig. 2, we have assumed a distance modulus for the Pleiades of $(m\text{-}M)_o$ = 5.53, and A_V = 0.12. This distance modulus corresponds to the "traditional" ZAMS-fitting distance to the Pleiades, and thus differs by $\sim$0.2 mag from the Hipparcos Pleiades distance modulus of 5.33 (Mermilliod et al.1997; van Leeuwen & Ruiz 1997). In practice, for this paper, the 0.2 mag uncertainty in the Pleiades distance modulus has no significant affect on any of our conclusions nor on the selection of objects that we believe to be good Pleiades brown dwarf candidates, and so our choice of which Pleiades distance to use should make no difference. The large filled dots in Fig. 2 are our Pleiades VLM and brown dwarf candidates. They were identified solely on the basis of their location in the color-magnitude diagram, i.e., close to the empirical field ZAMS scaled to the Pleiades distance. In pratice, the photometric candidates were empirically defined as having $I_c \leq 4.29(R_c - I_c) + 9.13$, except for CFHT-PL-26 which lies slightly bluer than this limit. The photometry and positions for these stars are provided in Table 3 (if the photometry is from CFHT) and Table 4 (if the photometry is from KPNO). Finding charts for the CFHT objects are provided in Fig. 4.

The data in the two tables allows us to make a few more statements about the external accuracy of our photometry and also to comment on a few interesting individual objects. We have photometry for three HHJ stars (the number is so few because our bright limit is such that most HHJ stars would be saturated in our images). The HHJ photometry for these three stars is listed in Tables 3 and 4. Unfortunately, these were not among the stars for which HHJ obtained CCD photometry, and the one sigma accuracy of their photographic photometry is only 0.1 to 0.2 mag. The agreement between our photometry and theirs for these three stars is satisfactory given the expected photometric accuracies. The photometry of Roque 7 and 16, Calar 3 and Teide 2 obtained by the IAC group (Zapatero-Osorio et al. 1997, Zapatero-Osorio, Rebolo, Martín –hereafter ZORM97–, Martín et al. 1998, cf. Table 3), appears to systematically differ from ours by $\sim$0.1-0.2 mag in the R and I-bands. One of our field also contains Calar 6 and 7. We get I_c = 19.290, $(R\text{-}I)_c$ = 2.13 for Calar 6 (19.20 and 2.59:, respectively, in ZORM97), and I_c = 19.831,$(R\text{-}I)_c$ = 1.73 for Calar 7 (19.7 and 2.52::, respectively, in ZORM97). From our photometry, these 2 objects appear to be background late-type stars, a conclusion also reached on the basis of low resolution spectroscopy by Martín et al.(1996). The two 2MASS objects with photometry from our KPNO images are apparently not Pleiades members based on their high proper motions (Kirkpatrick, Beichman and Skrutskie 1997); our photometry places them well above the locus of candidate Pleiades members, also suggesting that they are foreground very late type dwarfs. No accurate optical photometry of these two stars has been published, but our R-I colors are consistent with the spectral types of M8 and $>$M10 given by Kirkpatrick, Beichman and Skrutskie. Finally, a Pleiades brown dwarf candidate found in an I, Z survey by Cossburn et al.(1997) was also detected in our survey. This object, PIZ 1, has I_c = 20.22, $(R\text{-}I)_c$ = 2.2 according to our photometry. As such, it would not have been considered a brown dwarf according to our criteria - that is, it falls considerably blueward of the locus of stars we have identified as probable Pleiades members. PIZ 1 does, however, fall on a diffraction spike from a bright star on our I image and this may have affected our photometry (though the diffraction spike is much fainter than PIZ 1, and so we do not believe the effect on our photometry should be substantial).

In Fig. 5, we replot just the new candidate low mass Pleiades plus some other previously identified Pleiades stellar and brown dwarf members. The faintest two previously identified members are Teide 1 and Calar 3 (Zapatero-Osorio, Rebolo, and Martín 1997). It can be seen from inspection of Fig. 5 that our new proposed Pleiades VLM and brown dwarf candidates are located in the same region as the previously identified candidates (this was, of course, part of our reason for identifying these objects as new candidate Pleiades brown dwarfs).

In Fig. 6, we show the I-band luminosity function for the Pleiades. The data used to compute the stellar portion of the ILF are described in Sect. 3.3 below. The volume of the cluster is estimated to be 1230 pc^3 (3° radius) and the number of CFHT's VLM and brown dwarf candidates per magnitude bin has been scaled to the total number of HHJ Pleiades members as described in Sect. 3.3 for the mass function.

3.1. The estimated field star contamination

As should be obvious from Fig. 2, an I versus $(R\text{-}I)_c$ diagram cannot, of course, identify objects as certain Pleiades members. The most obvious alternative is that the objects we have identified in Table 3 could be instead low mass, field M dwarfs foreground to the Pleiades. If the theoretical models are approximately correct, and if the age of the Pleiades is $\sim$100 Myr, then VLM and brown dwarf Pleiades members should fall on an isochrone about 0.5 to 0.7 mag above the ZAMS, and hence the objects we have identified as single, Pleiades age, Pleiades distance brown dwarfs could also be slightly higher mass, main sequence, single, field M dwarfs located about 30% closer to us than the Pleiades. Allowance for the presence of binary stars in the Pleiades and in the field leads to a range of distances over which field M dwarfs could have the same apparent photometric properties as Pleiades brown dwarfs.

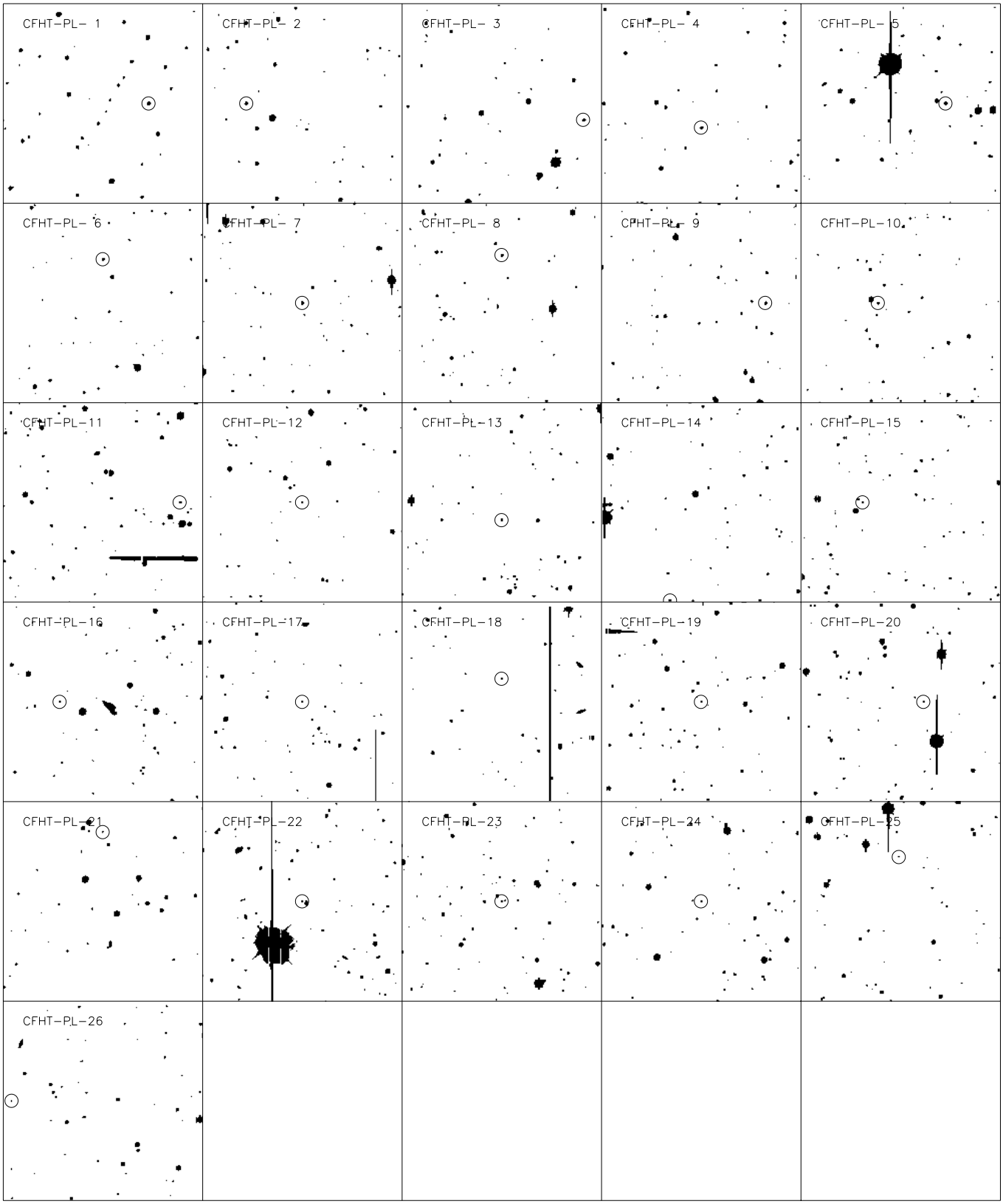

Fig. 4. Finding charts for objects listed in Table 3. Each panel is 210 arcsec on a side, North is up, East is left.

In order to try to assess the likely level of field star contamination in our sample of objects, we have made two simple calculations. For the first method, we assume that the Pleiades and the field star population have the same mass function and

Table 3. CFHT VLM stars and brown dwarfs candidates.

id	IAU	I_c	R_c-I_c	RA(2000) (h m s)	DEC(2000) (° ′ ″)	Prev. ID
CFHT-PL-1	VLC J0351516+233450	16.10	1.76	3:51:51.6	23:34:50.2	
CFHT-PL-2	VLC J0352443+235415	16.54	1.83	3:52:44.3	23:54:15.2	
CFHT-PL-3	VLC J0352518+233349	16.62	1.85	3:52:51.8	23:33:48.9	HHJ22, I=16.55, (R-I)=1.97
CFHT-PL-4	VLC J0353096+233348	16.76	1.89	3:53:09.6	23:33:48.3	
CFHT-PL-5	VLC J0348447+243723	17.03	2.00	3:48:44.7	24:37:22.7	
CFHT-PL-6	VLC J0352079+235915	17.11	2.33	3:52:07.9	23:59:14.6	
CFHT-PL-7	VLC J0352058+241732	17.34	1.94	3:52:05.8	24:17:31.7	
CFHT-PL-8	VLC J0342268+245021	17.42	2.00	3:42:26.8	24:50:21.3	
CFHT-PL-9	BDC J0349151+243622	17.71	2.18	3:49:15.1	24:36:22.4	
CFHT-PL-10	BDC J0344323+252518	17.82	2.21	3:44:32.3	25:25:18.2	
CFHT-PL-11	BDC J0347390+243622	17.91	2.21	3:47:39.0	24:36:22.1	Roque 16, I=17.79 (Zapatero-Osorio et al. 1997)
CFHT-PL-12	BDC J0353551+232337	18.00	2.47	3:53:55.1	23:23:37.4	
CFHT-PL-13	BDC J0352067+241601	18.02	2.21	3:52:06.7	24:16:01.4	Teide 2, I=17.82, (R-I)=2.23 (Martín et al. 1998)
CFHT-PL-14	BDC J0343142+242321	18.04	2.17	3:43:14.2	24:23:21.3	
CFHT-PL-15	BDC J0355125+231738	18.62	2.34	3:55:12.5	23:17:38.0	
CFHT-PL-16	BDC J0344352+251343	18.66	2.56	3:44:35.2	25:13:43.3	
CFHT-PL-17	BDC J0343001+244352	18.80	2.43	3:43:00.1	24:43:52.2	
CFHT-PL-18	BDC J0353231+231920	18.81	2.57	3:53:23.1	23:19:19.5	
CFHT-PL-19	BDC J0345331+253430	18.92	2.51	3:45:33.1	25:34:30.4	
CFHT-PL-20	BDC J0344127+252436	18.96	2.42	3:44:12.7	25:24:35.6	
CFHT-PL-21	BDC J0351256+234521	19.00	2.50	3:51:25.6	23:45:20.6	Calar 3, I=18.73, (R-I) = 2.54 (ZORM97)
CFHT-PL-22	BDC J0354594+235809	19.28	2.38	3:54:59.4	23:58:08.5	
CFHT-PL-23	BDC J0352186+240429	19.33	2.57	3:52:18.6	24:04:28.7	
CFHT-PL-24	BDC J0343402+243012	19.50	2.61	3:43:40.2	24:30:11.8	Roque 7, I=19.29 (Zapaterio-Osorio, priv. comm.)
CFHT-PL-25	BDC J0354053+233400	19.69	2.57	3:54:05.3	23:34:00.2	
CFHT-PL-26	BDC J0354014+244447	20.21	2.56	3:54:01.4	24:44:47.1	

Table 4. KPNO VLM stars and brown dwarfs candidates.

id	IAU	I_c	R_c-I_c	RA(2000) (h m s)	DEC(2000) (° ′ ″)	Prev. ID
CFHT-PL-2	VLC J0352443+235415	16.61	1.79	3:52:44.3	23:54:15.2	
CFHT-PL-5	VLC J0348447+243723	17.02	1.97	3:48:44.7	24:37:22.7	
CFHT-PL-10	BDC J0344323+252518	17.78	2.14	3:44:32.3	25:25:18.2	
CFHT-PL-12	BDC J0353551+232337	17.97	2.56	3:53:55.1	23:23:37.4	
KPNO-PL-1		15.82	2.47	3:54:01.3	23:16:35.4	2MASS J0354012+231635
KPNO-PL-2		17.45	2.46	3:45:43.0	25:40:23.8	2MASS J0345432+254023
KPNO-PL-3	VLC J0354011+231942	16.67	1.77	3:54:01.1	23:19:42.0	HHJ 20, I=16.59, (R-I)=1.52
KPNO-PL-4	VLC J0353480+234911	16.45	2.05	3:53:48.0	23:49:10.5	HHJ 28, I=16.43, (R-I)=2.01
KPNO-PL-5	VLC J0349567+245909	17.35	2.01	3:49:56.7	24:59:08.9	

that the field star mass density in the solar neighborhood is 0.05 $\mathcal{M}_\odot$/pc^3 (c.f. Allen 1973). If the distance range where field stars can mimic Pleiades brown dwarfs is 60 to 125 pc, and given that we have surveyed a 2.5 square degree region, the volume from which interlopers could be drawn is about 450 pc^3; the mass of field stars in such a region should then be about 23 $\mathcal{M}_\odot$. This is to be compared with the total mass of Pleiades members over the area we surveyed. Estimating what fraction of the Pleiades we have surveyed is difficult to do with precision. As a first estimate, somewhat arbitrarily assume a total "area" for the Pleiades of 30 square degrees, corresponding for a circular cluster to a radius of about 3 degrees. This is much larger than the largest area, faint proper motion survey of the Pleiades obtained to date, and the 3 degree radius is about five times the core radius or 3.5 times the estimated half-mass radius for the Pleiades (Raboud & Mermilliod 1998) - thus we believe this is a very conservative assumption. With this assumed cluster area, our 2.5 square degree CFHT survey would cover 8.3% of the Pleiades. To be somewhat more quantitative, we have made the following calculation using data from the Hambly, Hawkins and Jameson (1993) proper motion survey for low mass Pleiades members. For each of our CFHT fields, we have determined the

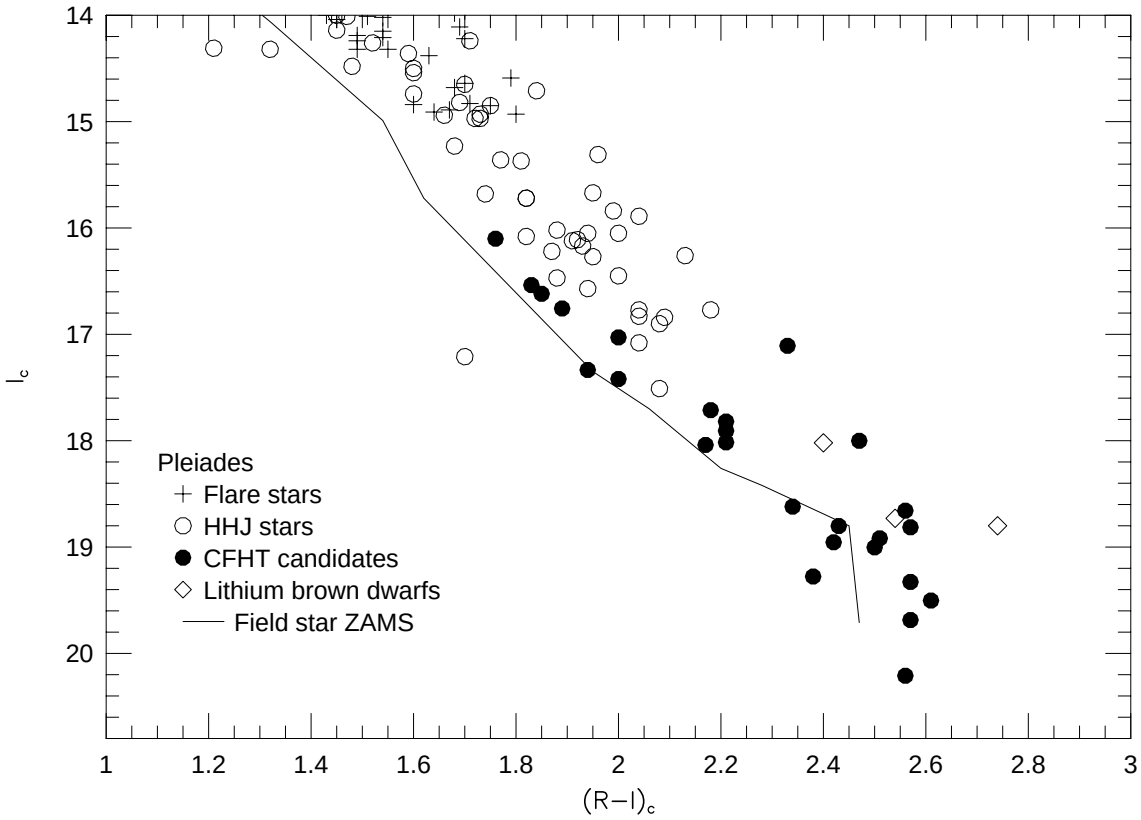

Fig. 5. Color-magnitude diagram for the faint end of the Pleiades main sequence and our new brown dwarf sequence. The different symbols are identified in the lower-left corner of the figure. The solid piece-wise curve is an empirical field star ZAMS shifted to Pleiades distance and reddening derived from the Cousins system photometry for Gliese catalog M dwarfs provided by Leggett (1992).

minimum and maximum radial distance from the center of the Pleiades covered by the image, and we have then determined the number of stars in the HHJ catalog in this radial distance range. Combining these data, we can then estimate the number of HHJ Pleiades members that on average would have been included in a survey like ours. We derive an estimated 53 HHJ stars from this procedure, corresponding to roughly 12% of the total HHJ catalog. Since the total area surveyed by HHJ was of order 20 square degrees, our derived fraction is essentially just what we would have gotten making no assumptions about the radial distribution of our fields. We must correct this estimate for the Pleiades members outside the region surveyed by HHJ. Simply scaling from the area surveyed by HHJ to our assumed 30 square degree total cluster area brings us back again to an estimate that our CFHT survey would have included of order 8% of the Pleiades. The total dynamical mass of the Pleiades is in the range 700-1100 $\mathcal{M}_\odot$(van Leeuwen 1983; Jones 1970). Taking the lower of these estimates, we then conclude that on average our fields would have included about 56 $\mathcal{M}_\odot$ of Pleiades members. Compared to the 23 $\mathcal{M}_\odot$ of field dwarfs in our survey area, this suggests that of order 70% of our brown dwarf candidates are likely to be Pleiades members.

The second method for estimating the possible field star contamination of our sample is more straightforward. The field star luminosity function, as estimated from the DENIS survey (Delfosse 1997), for the color range spanned by our brown dwarf candidates indicates that it can be approximated as a constant, $\Phi(I) \sim 0.003$ stars/pc^3 per magnitude in I. With our survey volume of 450 pc^3, we predict of order 1.3 field dwarfs per one magnitude bin in I, or about 4 field stars in the $17 < I_c < 20$ magnitude range covered by our brown dwarf candidates - corresponding to an ∼80% "success" rate. The two methods therefore are in reasonable agreement, and suggest that perhaps 75% of our brown dwarf candidates should be true Pleiades members.

As a final indication that the majority of our brown dwarf candidates are likely to be Pleiades members, we note that our candidates are concentrated towards the center of the cluster as would be expected of members but not of field stars. This is illustrated in Fig. 7. To construct this figure, we split each CFHT field into one square arcminute bins, and derived the total area surveyed at CFHT as a function of radial distance from the cluster center. We combined these data with the radial locations of our brown dwarf candidates to derive the surface density of candidates as a function of radial distance from the cluster center. As expected, the histogram suggests that the highest surface density for brown dwarfs should be at the cluster center. We have no data for $r \leq 0.5$ degrees because the Pleiades B stars and the prominent reflection nebulosity make this region extremely inhospitable for deep optical imaging.

Stauffer, Schultz & Kirkpatrick (1998) recently obtained intermediate resolution spectra of 7 CFHT-PL candidates. All

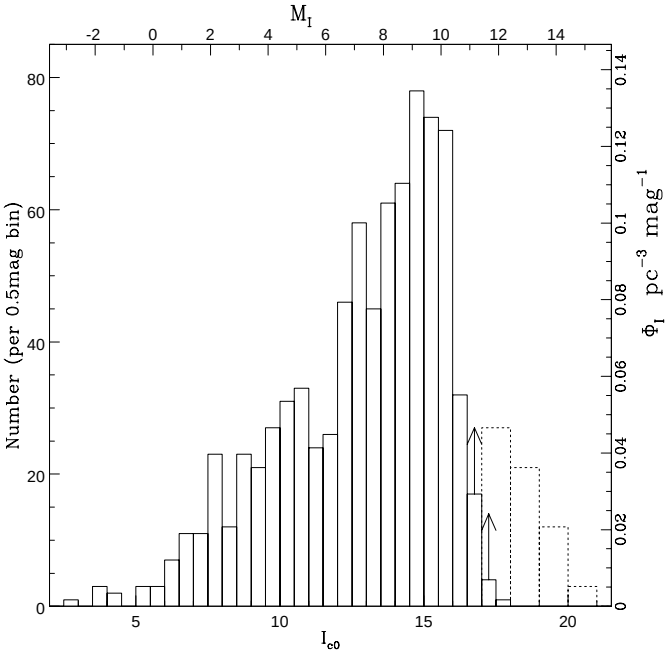

Fig. 6. The I-band luminosity function of Pleiades members. The CFHT VLM and brown dwarf candidates are shown as the dashed histogram. The last 2 bins of the solid histogram are lower limits due to the incompleteness of the HHJ survey. The first bin of the dashed histogram may also be incomplete due to the saturation limit of the CFHT survey. This luminosity function takes no account of binarity.

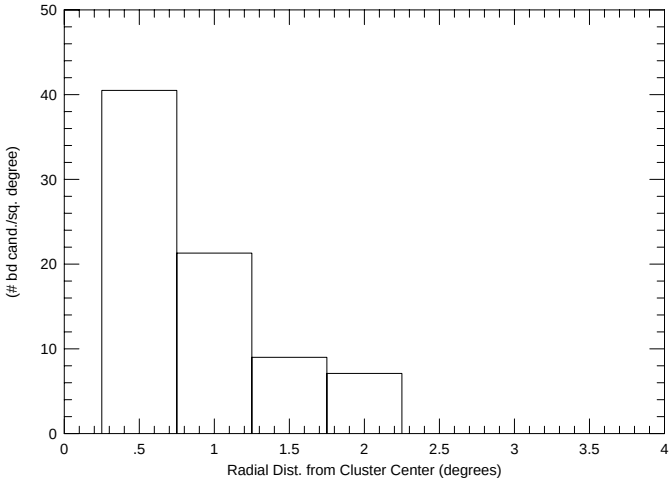

Fig. 7. The radial surface density distribution for the brown dwarf candidates from our survey. Because of the small number of objects, the detailed shape of the distribution is not well determined, but we believe the concentration to the cluster center is real, and indicative that most of our candidate objects are indeed Pleiades members.

except one (CFHT-PL-14) have radial velocities consistent with membership, H_α emission, and spectral types of M6.5 or later. Among the 5 observed candidates with $I_{c0} > 17.8$, all except CFHT-PL-14 exhibit lithium in absorption. This result is consistent with the low contamination level of the CFHT-PL sample by field stars estimated above from photometry.

3.2. Estimated masses for the brown dwarf candidates

To derive estimated masses for the stars of Table 3, we adopt the following procedure. First, we assume that HHJ 3 defines the faint end of the lithium 'chasm" in the Pleiades (i.e. the point faintward of which Pleiades members will begin to show appreciable lithium, and brightward of which they have no remaining lithium). It is unlikely that the edge of the lithium chasm is significantly brighter than HHJ 3, since there are several other Pleiades members only slightly brighter than HHJ 3 that have also been determined not to have detectable lithium. Because PPL 15 may be a nearly equal mass binary (Basri & Martín 1998), it is possible that the edge of the lithium chasm could be several tenths of a magnitude fainter than HHJ 3. If this were the case, however, the inferred age of the Pleiades (see below) would be even older than 120 Myr which would conflict with upper-main sequence ages for the cluster. Second, we adopt several approximately "current-generation" theoretical evolutionary tracks from Baraffe et al.(1998, BCAH98), Burrows (1998, B98), and D'Antona & Mazzitelli (1998, DAM98). We adopt an age for each model such that the lithium edge (defined here as the 90% depletion point) corresponds to the absolute I magnitude (BCAH98) or to the bolometric luminosity (B98, DAM98) of HHJ 3. For all three sets of models, this age is within 5 Myr of 125 Myr. The most straightforward method to get mass is then to use the $M_I - Mass$ relationship for an age of 120 Myr from BCAH98's model. The masses thus obtained are listed in column 3 of Table 5. We also used the $M_{bol} - Mass$ relationships from B98 and DAM98 models. The Monet et al.(1992) bolometric conversions were used to determine M(Bol) from $M(I_c)$ and $(R\text{-}I)_c$ and the calculated masses are also provided in Table 5. Even though the second method is more uncertain due in part to the hazardous estimate of bolometric correction for brown dwarfs, the masses derived by the 2 methods are very similar. In the following, we use the masses derived from the BCAH98 model.

With these mass calibrations, we have 17 objects from our survey whose masses are below the HBML if they are Pleiades members and if the models are correct. The lowest mass objects that we have identified have masses of order 0.045 $\mathcal{M}_\odot$. The method by which we have estimated masses is in principle only correct for single stars; for equal mass binaries, this method would overestimate the masses of the individual components of the binary system by of order 0.01 to 0.03 $\mathcal{M}_\odot$in this mass range. The location in Fig. 5 of CFHT-PL-6 and CFHT-PL-12 suggest that they are likely to be nearly equal mass binaries if they are indeed Pleiades members.

3.3. The Pleiades mass function

Now that we have a survey which extends well into the brown dwarf regime and covers a significantly large fraction of the total cluster area, it becomes possible to estimate the mass function of the Pleiades to below the HBML. We will make such an estimate in this section; however, we note that even with this much improved data, there are many sources of systematic errors which

Table 5. MASS ESTIMATES FOR VLM AND BD CANDIDATES

		Mass($M_\odot$)			Mass($M_\odot$)	
Object	$M(I_c)$	BCAH'98	$(R-I)_{c,0}$	M(Bol)	D'A&M'98	Burrows'98
CFHT-PL-1	10.51	0.140	1.73	10.813	0.138	0.130
CFHT-PL-2	10.95	0.115	1.80	11.192	0.110	0.109
CFHT-PL-3	11.03	0.112	1.82	11.256	0.105	0.106
CFHT-PL-4	11.17	0.106	1.86	11.357	0.099	0.101
CFHT-PL-5	11.44	0.097	1.97	11.514	0.090	0.093
CFHT-PL-6	11.52	0.094	2.30	11.137	0.113	0.112
CFHT-PL-7	11.75	0.087	1.91	11.885	0.074	0.077
CFHT-PL-8	11.83	0.084	1.97	11.905	0.073	0.076
CFHT-PL-9	12.12	0.076	2.15	11.969	0.070	0.074
CFHT-PL-10	12.23	0.073	2.18	12.034	0.068	0.071
CFHT-PL-11	12.32	0.071	2.18	12.121	0.065	0.068
CFHT-PL-12	12.41	0.070	2.44	11.786	0.078	0.081
CFHT-PL-13	12.43	0.069	2.18	12.230	0.062	0.064
CFHT-PL-14	12.45	0.069	2.14	12.310	0.060	0.061
CFHT-PL-15	13.03	0.059	2.31	12.632	0.052	0.051
CFHT-PL-16	13.07	0.059	2.53	12.271	0.061	0.063
CFHT-PL-17	13.21	0.057	2.40	12.660	0.052	0.051
CFHT-PL-18	13.22	0.057	2.54	12.407	0.057	0.058
CFHT-PL-19	13.33	0.056	2.48	12.628	0.053	0.052
CFHT-PL-20	13.37	0.055	2.39	12.831	0.049	0.046
CFHT-PL-21	13.41	0.055	2.47	12.732	0.051	0.049
CFHT-PL-22	13.69	0.052	2.35	13.222	0.044	0.038
CFHT-PL-23	13.74	0.051	2.54	12.921	0.048	0.044
CFHT-PL-24	13.91	0.050	2.58	13.015	0.046	0.042
CFHT-PL-25	14.10	0.048	2.54	13.279	0.044	0.037
CFHT-PL-26	14.62	0.044	2.53	13.823	0.039	0.031

will in principle lend uncertainty to this estimate. Those difficulties include: mass segregation and the preferential loss of low mass stars during cluster evolution, the effect of binaries on the shape of the mass function (Kroupa 1995), incompleteness in the proper motion surveys for the higher mass stars and the imaging surveys for the low mass objects, remaining uncertainties in the theoretical models used to convert the observations to masses and uncertainties in the age and distance to the Pleiades. Most of these effects act in the direction to cause us to underestimate the number of low mass stars and brown dwarfs, so in some sense our estimated mass function can be regarded as a lower limit to the true Pleiades mass function.

For the stellar portion of the IMF, we have constructed a catalog of probable Pleiades members derived from proper motion surveys by Hertzsprung (1947), Trumpler (1921), Pels, Oort, & Pels-Kluyver (1985), Artyukhina & Kalinina (1970), Stauffer et al.(1991), and Hambly, Hawkins & Jameson (1993). To be included in the catalog, in addition to the proper motion membership we require that there also be either accurate radial velocities or photometry (and preferably both) which confirm membership (e.g. van Leeuwen, Alphenaar & Brand 1986; Rosvick, Mermilliod & Mayor 1992a,b; Prosser, Kraft & Stauffer 1991 and references therein). This catalog contains 810 stars.

Because of the heterogeneous nature of the data available for these 810 stars, we have adopted a somewhat approximate technique to estimate masses. In particular, some of the stars have only photographically determined colors. We have therefore chosen to adopt bolometric corrections that are a function of absolute magnitude rather than color (we have done so in a way, however, that accounts for the pre-main sequence nature of the Pleiades stars). For the B through early-K dwarfs of the cluster, down to $0.7 M_\odot$, we use a polynomial fit to the bolometric corrections from Schmidt-Kaler (1982). To convert from M(bol) to mass, we use a 120 Myr isochrone from D'Antona & Mazzitelli (1998). For the late-K and M dwarfs and in the substellar domain, we used BCAH98's 120 Myr isochrone to derive masses, in the 0.03–0.7 $M_\odot$ range, from the $M_I - Mass$ relationship.

We use only our CFHT data to estimate the mass function below the HBML, in order to make as few assumptions as possible with respect to mass segregation, completeness, etc. We assume that the radial distribution of stars less massive than the HBML in the Pleiades is the same as for stars with $15.0 < I < 16.5$ (the faintest stars for which the HHJ survey is nearly complete, corresponding roughly to 0.15 to 0.25 $\mathcal{M}_\odot$). Based on the location and size of our CFHT fields, more than 85% of the area we have surveyed is located between 0.75 and 1.75 degrees from the center of the Pleiades. Thirty-nine percent of the HHJ stars between I = 15 and I = 16.5 fall in that same radial distance range. To scale our counts of brown dwarf candidates to the full HHJ survey area, we then multiply the number of CFHT objects by three factors: (a) the ratio of the annular area between 0.75 and 1.75 degrees to our CFHT survey area of 2.5 sq. degrees; (b) the ratio of the total number of $15 < I < 16.5$

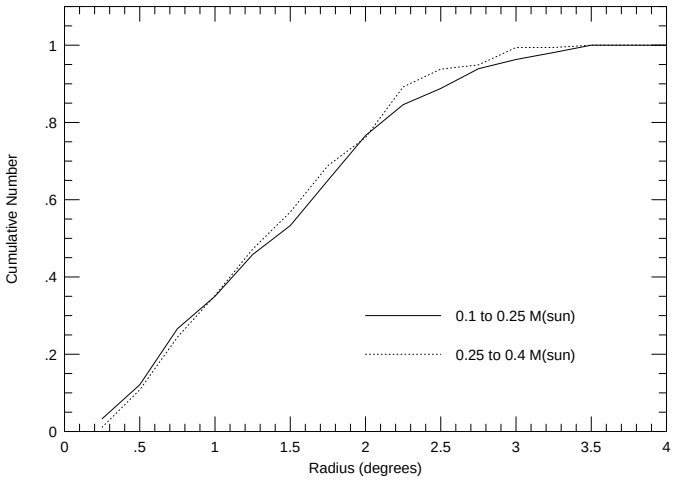

Fig. 8. The cumulative radial distribution of stars from the HHJ catalog for the mass ranges 0.13 to 0.25 $\mathcal{M}_\odot$ and 0.25 to 0.4 $\mathcal{M}_\odot$.

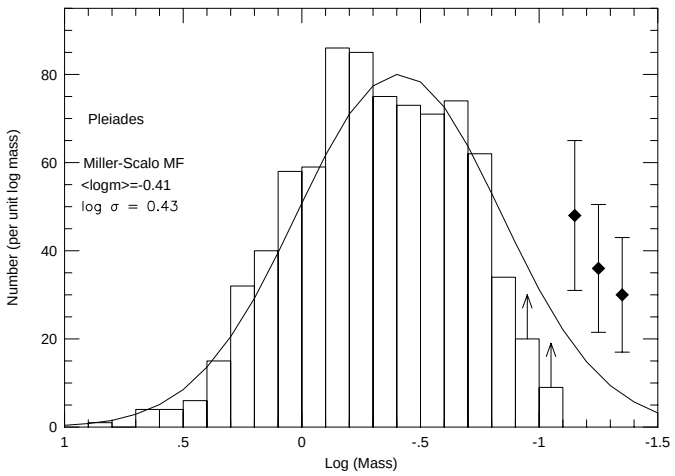

Fig. 9. The Pleiades mass function represented in terms of logarithmic mass intervals. The histogram represents Pleiades members as cataloged from published proper motion surveys; the three diamonds and associated error bars are derived from our survey. See the text for details.

stars in the HHJ catalog to those in this annular region, and (c) the estimated fraction of our brown dwarf candidates that are indeed Pleiades members. The correction factor turns out to be basically 6.0. In principle, there should also be a correction for the relative incompleteness of the HHJ survey compared to our survey. HHJ estimate their completeness as ∼70%, mostly due to blended images or regions "burned-out" by bright stars. We have estimated our completeness in the magnitude range of interest as ∼90%, but this is an internal completeness from comparison of separate images of the same region. We also will miss objects that are blended with another star, or that are near bad-columns or charge-overflow columns, or are near the edge of the CCD. We therefore prefer not to make a relative completeness correction since the magnitude of the correction is too uncertain.

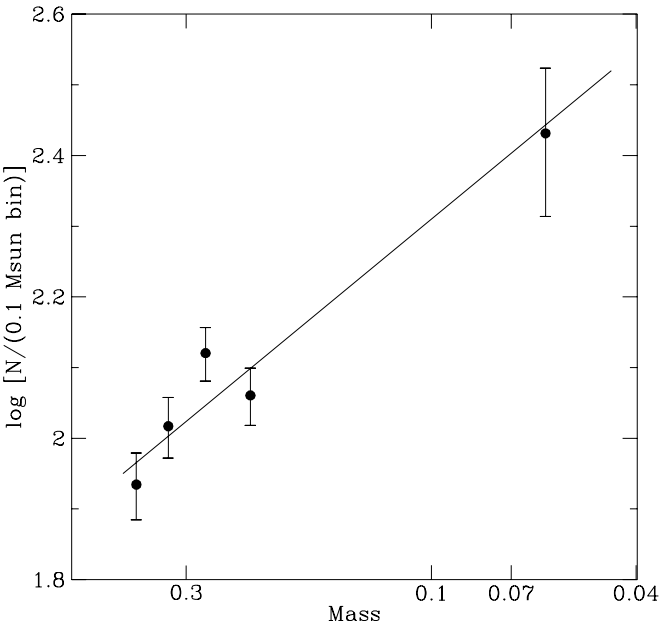

Fig. 10. The Pleiades mass function represented in terms of linear mass intervals, for M $< 0.4\ \mathcal{M}_\odot$.

We justify our assumption that the radial distribution for objects below the HBML is not greatly different from that for ∼0.2 $\mathcal{M}_\odot$ Pleiades members by comparing the radial distribution for the ∼0.2 $\mathcal{M}_\odot$ HHJ stars to HHJ stars of about twice this mass. This is done in Fig. 8, which shows the cumulative radial distribution for 0.25 to 0.4 $\mathcal{M}_\odot$ Pleiades and 0.13 to 0.25 $\mathcal{M}_\odot$ Pleiades. The two distributions are not discernibly different. From this we conclude that any increase in core or half-mass radius with decreasing stellar mass is only a relatively weak function of mass, and that we do not greatly underestimate the brown dwarf population in the Pleiades by assuming it is distributed like the 0.2 $\mathcal{M}_\odot$ Pleiades members.

We present our derived mass function for the Pleiades in two formats. First, in Fig. 9 as the estimated number of stars per logarithmic mass interval, and second in Fig. 10 as the number of stars per 0.1 $\mathcal{M}_\odot$ bin. Fig. 9 suggests that the Pleiades mass function is reasonably well approximated by a log-normal distribution (c.f. Miller & Scalo 1979), except below the HBML where there are more objects than predicted by the log-normal distribution. Fig. 10 shows that when considered in terms of linear mass bins, the Pleiades mass function is still rising below the HBML though more shallowly than the Salpeter exponent. The line shown in Fig. 10 corresponds to dN/dM $\sim$ M$^{-0.6}$. Taking into account the error bars associated to the estimated number of brown dwarf candidates in Fig. 10, the 1σ uncertainty on the power–law exponent is 0.15 dex.

From a compilation of independent photometric surveys covering different areas of the cluster in various filters and reaching limiting magnitudes in the range from I=19.0 to I=21.6, Martín et al. (1998) recently derived a slightly steeper power–law mass function in the 0.04-0.25 M$_\odot$ range, with an exponent of -1.0±0.15 (1σ). The method they used to correct for con-

tamination of the candidate members by field dwarfs, whose amount may vary from one survey to the other depending on the location of the surveyed area relative to the cluster's center and on the filters used, differs from ours especially in the way of estimating the radial distribution of low–mass objects in the cluster. Therefore, even though their result formally differs from ours at the 2.7σ level, we believe that this difference may not be statistically significant.

Extrapolating the power-law mass function shown in Fig. 10 to 0.01 $\mathcal{M}_\odot$ we predict there should be at least 250 brown dwarfs in the Pleiades. However, because of their small individual masses, this does not indicate a large contribution to the total mass of the Pleiades from objects below the HBML. Integrating our power-law mass function, we derive a total mass in brown dwarfs of only about 10 $\mathcal{M}_\odot$, corresponding to about 1 to 1.5% of the mass of the Pleiades. Though numerous, brown dwarfs have therefore a negligeable influence on the dynamical evolution of the cluster.

4. Conclusion

We have identified seventeen brown dwarf candidates in the Pleiades, with the faintest having a mass of order 0.045 $\mathcal{M}_\odot$based on current models. Based on predictions of the field star densities, and also based on our previous success rate in confirming photometric brown dwarf candidates in the Pleiades, we estimate that of order 70% of these candidates will indeed turn out to be Pleiades members (and hence that they are likely brown dwarfs of age $\sim$ 120 Myr). We have also obtained photometry of two objects previously confirmed as Pleiades brown dwarfs – Calar 3 and Teide 2–, and of three previously identified brown dwarf candidates – Roque 7 and 16, PIZ 1–. Our photometry agrees within 0.1-0.2 mag with previously published photometry, except for PIZ 1 for which our photometry suggests that it is significantly bluer than other Pleiades brown dwarf candidates of the same I magnitude. This may indicate that PIZ 1 is not a member of the Pleiades, despite its very late spectral type (Cossburn et al 1997). If PIZ 1 is a Pleiades member, and if our R-I color for it is reasonably accurate, then we may have underestimated the number of Pleiades brown dwarfs because the boundary between the VLM field stars and the Pleiades locus is bluer than we had thought. This could also account for the fact that, beyond (R-I)=2.55, we do not find any Pleiades BDC candidate even though our completeness limit lies at (R-I)$\sim$3.0.

With our current estimate of the number of Pleiades brown dwarfs, we predict that objects below the hydrogen burning mass limit make up only a few per cent of the mass of the Pleiades. This estimate is uncertain due primarily to lack of verification that our identified objects are actually Pleiades members and due to the relatively small fraction of the cluster that we have surveyed. The most certain way to verify that our candidate objects are brown dwarfs (and Pleiades members) would be to obtain red spectra of sufficient signal-to-noise to measure the lithium λ6708Å equivalent width (and/or to measure an accurate radial velocity). At present this is only possible with the Keck telescopes due to the faintness of these stars, although within a few years other large telescopes should become available which will be capable of spectroscopy of sufficient sensitivity. In any case, even with large telescopes, useful spectroscopy is unlikely to be possible for objects fainter than I $\simeq$ 19.5. The next best way to verify Pleiades membership - and which should be good to at least I $\sim$ 21 - would be to determine accurate proper motions for our candidate objects. Due to the good seeing and small pixel size for the CFHT images, this should become possible in only of order five years since the Pleiades motion is about 0.05 arcsec per year. In the near future, it will be useful to obtain near-IR photometry for all of the candidate objects in order to confirm that their colors are compatible with the predicted effective temperatures for Pleiades brown dwarfs. This is particularly necessary because of the possible saturation of the $(R\text{-}I)_c$ color index for our faintest stars. We expect that infrared color indices will not saturate, and so there will be a better separation of the Pleiades brown dwarfs from possible field star contaminants once we have a broader wavelength coverage for our photometry.

Acknowledgements. We gratefully acknowledge the guidance of Jean-Charles Cuillandre for the reduction of the UH8K images and the help of Christian Veillet for the astrometric calibration of the frames. We thank I. Baraffe, A. Burrows, G. Chabrier, and F. D'antona for making their models available to us before publication. JRS gratefully acknowledges support from NASA via grants NAGW-2698 and NAG5-3363.

References

Allen C.W. 1973, Astrophysical Quantities, 3rd edition.
Artyukhina N., Kalinina E. 1970, Tr. Shternberg Astron. Inst. 39, 111
Baraffe I., Chabrier C., Allard F., Hauschildt P.H. 1998, AA, submitted (BCAH98)
Basri G., Martín E.L. 1998, in: Brown Dwarfs and Extrasolar Planets, eds. R. Rebolo, E. L. Martín and M. R. Zapatero-Osorio, ASP Conf. Series, Vol. 134, p. 284
Basri G., Marcy G., Graham J. 1996, ApJ 458, 600
Bertin E., Arnouts S. 1996, A&AS 117, 393.
Bessell M. 1990, A&AS 83, 357
Burrows A. 1998, priv. comm (B98)
Burrows A., Marley M., Hubbard W.B. et al.1997, ApJ 491, 856
Cossburn M.R., Hodgkin S.T., Jameson R.F., Pinfield D.J. 1997, MNRAS 288, L23.
Cuillandre J.-C., Mellier Y., Dupin J.-P., Tilloles P., Murowinski R., Crampton D., Wolff R., Luppino G. 1996, PASP 108, 1120.
D'Antona F., Mazzitelli I. 1998, priv. comm. (DAM98)
Delfosse X. 1997, Ph. Thesis, Université de Grenoble
Festin L. 1997, AA 322, 455
Hambly N.C., Hawkins M.R.S., Jameson R.F. 1993, A&AS 100, 607
Hertzsprung E. 1947, Ann. Sterrew. Leiden 19, 3
Jameson R.F., Skillen I. 1989, MNRAS 239, 247
Jones B.F. 1970, AJ 75, 563
Kirkpatrick J.D., Beichman C.A., Skrutskie M.F. 1997, ApJ 476, 311
Kroupa P. 1995, ApJ 453, 358
Landolt A. 1992, AJ 104, 340.
Leggett S. 1992, ApJS 82, 351
Lequeux J., Fort B., Dantel-Fort M., Cuillandre J.-C., Mellier Y. 1996, A&A 312, L1.
Marcy G., Basri G., Graham J. 1994, ApJ 428, L57

Martín E.L., Rebolo R., Magazzù A. 1994, ApJ 436, 262
Martín E.L., Rebolo R., Zapatero-Osorio M.R. 1996, ApJ 469, 706
Martín E.L., Basri G., Gallegos J.E., Rebolo R., Zapatero-Osorio M.R., Béjar V.J.S. 1998, ApJ, in press
Mermilliod J.C., Turon C., Robichon N., Arenou F., Lebreton Y. 1997, in the Proceedings of the Venice Hipparcos meeting, M. Perryman (ed.), in press
Miller G., Scalo J. 1979, ApJS 41, 513
Monet D.G., Dahn C.C., Vrba F.J. et al.1992, AJ 103, 638
Oppenheimer B., Basri G., Nakajima T., Kulkarni S. 1997, AJ 113, 296
Pels G., Oort J., Pels Kluyver H. 1985, AA 43, 423
Prosser C., Kraft R., Stauffer J. 1991, AJ 101, 1361
Raboud D., Mermilliod J.-C. 1998, AA 329, 101
Rebolo R., Martín E., Magazzù A. 1992, ApJ 389, L83
Rebolo R., Martín E.L., Basri G., Marcy G. Zapatero-Osorio M.R. 1996, ApJ 469, L53
Rosvick J., Mermilliod J.-C., Mayor M. 1992a, AA 255, 130
Rosvick J., Mermilliod J.-C., Mayor M. 1992b, AA 259, 720
Schmidt-Kaler T.H. 1982, Physical Parameters of the Stars, in Landolt-Bornstein New Series, v. 2b (ed. K. Schaifers, H.H. Vogt). New York: Springer-Verlag.
Simons D.A., Becklin E.E. 1992, ApJ 390, 431
Stauffer J., Klemola A., Prosser C., Probst R. 1991, AJ 101, 980
Stauffer J., Hamilton D., Probst R. 1994, AJ 108, 155
Stauffer J., Hamilton D., Probst R., Rieke G., Mateo M. 1989, ApJ 344, L21
Stauffer J., Schultz G., Kirpatrick J.D., 1998, ApJ Letters, in press
Stauffer J., Giampapa M., Liebert J., Hamilton D. 1994, AJ 108, 160.
Stauffer J., Schild R., Barrado y Navascues D., Backman D., Angelova A., Kirkpatrick J.D., Hambly N., Vanzi, L. 1998, ApJ in press.
Trumpler R. 1921, Lick Obs. Bull. 10, 333.
van Leeuwen F. 1983, Thesis, Leiden.
van Leeuwen F., Alphenaar P., Brand J. 1986, AAS 65, 309
van Leeuwen F., Ruiz M. 1997, in the proceedings of the Venice Hipparcos meeting.
Williams D.M., Boyle R.P., Morgan W.T., Rieke G.H., Stauffer J.R., Rieke M.J. 1996, ApJ 464, 238
Zapatero-Osorio M., Rebolo R., Martín E.L. 1997, A&A 317, 164 (ZORM97)
Zapatero-Osorio M., Rebolo R., Martín E. et al.1997, ApJ 491, L81
Zapatero-Osorio M. et al.1998, in 'Brown Dwarfs and Extrasolar Planets', ASP Conf. Ser., R. Rebolo, E.L. Martin, M.R. Zapatero-Osorio, Vol. 134, p. 51